Ice and the apparent variation of GPS station positions for Alaska

by

Kelly Anne Kochanski

Submitted to the Department of Earth, Atmospheric and Planetary Sciences
in partial fulfillment of the requirements for the degree of

Bachelor of Science

at the

MASSACHUSETTS INSTITUTE OF TECHNOLOGY

June 2015

Author .....
Department of Earth, Atmospheric and Planetary Sciences
May 27, 2015

Certified by .....
Thomas Herring
Professor of Geophysics
Thesis Supervisor

Accepted by .....
Richard P. Binzel
Professor of Planetary Sciences

Ice and the apparent variation of GPS station positions for Alaska

by

Kelly Anne Kochanski

Submitted to the Department of Earth, Atmospheric and Planetary Sciences
on May 27, 2015, in partial fulfillment of the
requirements for the degree of
Bachelor of Science

Abstract

Many GPS stations in Alaska have apparent seasonal variations with amplitudes between 5 and 10mm. This motion is usually in phase with regional snowfall and has been attributed to hydrological loading (Fu et. al., 2012). We studied the phase of vertical seasonal motion for fifty stations in the PBO network across Alaska and Washington State and found six stations which move two to four months out of phase with snowfall with amplitudes greater than 4mm. The mean date at which stationsâĂŹ seasonal movement reached peak height was October 21st with a standard deviation of 49.7 days. 59% of this variation is created by the six stations with phases furthest from the mean. These stations are also distinguished by discontinuous winter movements, including jumps of more than 10mm/day, and they have the six most asymmetric time-series in the study. Three of these stations, AB11, AB12, and AB14, are local high points on AlaskaâĂŹs west coast. These locations have high wind speeds and humidity and we expect that in freezing conditions they accumulate thick frost and rime. This hypothesis is supported by multipath values at the sites, which show increased signal scattering during the winter. We used a simulation to demonstrate that signal delay in horizontal ice features such as rime can cause apparent vertical motion of GPS stations and found that the magnitude of the movement was determined by ice thickness and orientation. The apparent vertical seasonal motion of these stations is not caused by loads but is an artefact of signal delay from ice accumulation.

Thesis Supervisor: Thomas Herring
Title: Professor of Geophysics

Acknowledgments

The Plate Boundary Observatory, funded by NSF and by NASA, for collecting and processing GPS data. Weather Underground for providing weather records. Google Earth for curating satellite imagery.

Thomas Herring (MIT) for critical discussions about the project, as well as code for the plots of satellite positions. Jane Connor (MIT) for advice and discussions about the structure and presentation of this paper.

Andrei Klishin, James Logan and MIT La Maison Française for personal support and occasional bursts of scientific insight. You were crucial to the completion of this thesis, as for every other project I've worked on since I've known you.

Chapter 1

Introduction

The Plate Boundary Observatory (PBO) maintains a network of 1100 GPS stations across the western United States, each of which generates continuous time-series of the sites' positions. These time series commonly include seasonal signals. These annual displacements can be as large as several centimeters. A sample time series with seasonal oscillations is shown in Fig. 1-1. This is for station AB44, located in southeastern Alaska at 59.5°N, 135.2°W. The gap in this time series is a temporary maintenance issue. The power spectrum for this station, obtained by a Fourier transform, is shown in Fig. 1-2. The gap in the time series was filled by a quadratic interpolation. This fourier transform shows strong peaks for signals with yearly and half-yearly periods, sot the stations' periodic variation is predominantly annual and semi-annual.

Seasonal variations are interesting for two reasons. First, they offer insight into seasonal climactic and geophysical processes. For example, GPS measurements can be affected by mass redistribution during snowfall and glacial surges. Borsa, Agnew and Cayan (2014) also used GPS displacements to measure subsidence across the California Valley due to groundwater draining during the ongoing drought, and Flouzat et. al. (2009) used horizontal displacements to measure seasonal changes in geodetic strain in the Himalaya.

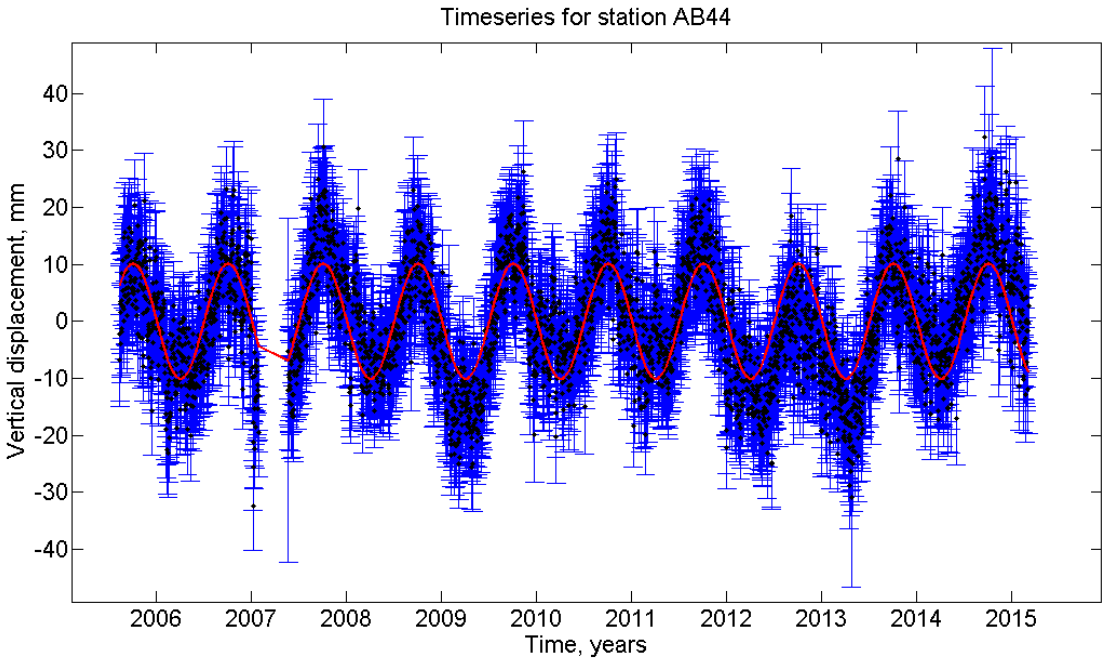

Figure 1-1: Detrended time-series of vertical displacement of PBO station AB44 with a best-fit curve for yearly variations.

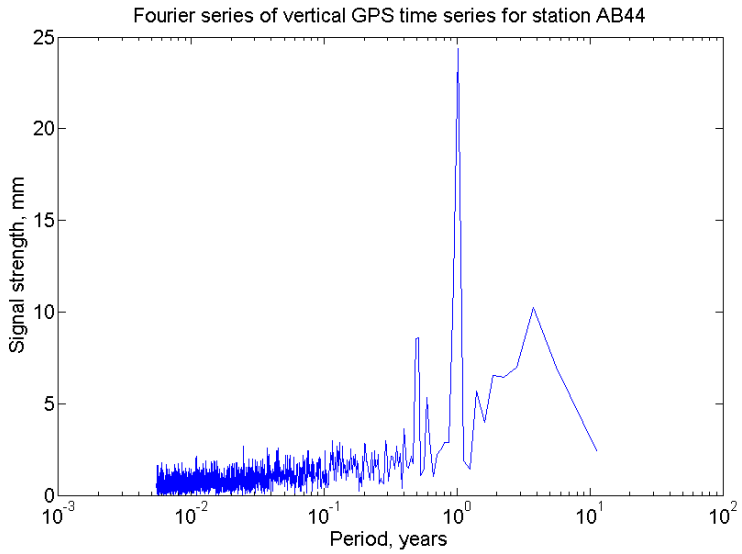

Figure 1-2: Power spectrum for the vertical time-series of station AB44.

Dong et. al. (2002) investigated these seasonal variations by looking for mass redistribution processes which would regularly load and unload the crust, causing the small seasonal uplifts observed by the GPS stations. They observed 4.5 years of continuous data from the United States and Japan, and explained approximately 66% of the seasonal variation by a combination of pole tide effects. atmospheric loading due to pressure variations, groundwater loading, snow mass and nontidal ocean mass. These effects each make contributions on the order of 5mm to the seasonal variation, depending on the local climate. Smaller effects on the order of 0.5mm are attributed to ocean tidal loading, bedrock thermal expansion, and network errors.

These estimates are limited by our knowledge of mass fluxes. Snow cover and groundwater are particularly difficult to estimate remotely. Authors including Tsai (2010) have attempted to remedy this by analyzing GPS data alongside other remote sensing techniques. For example, Tsai (2011) models both GPS positions and seismic velocities as functions of thermoelastic and hydrological variations. He finds that thermoelastic strains explain no more than 25% of GPS variations. Hydrology-induced variations, such as variations in poroelasticity, could explain the full amplitude of GPS seaonal variations without contradicting seismological models, though he does not attempt to use hydrological data to confirm this hypothesis.

Chapter 2

Seasonal variation of vertical GPS station measurements in Alaska

Alaska encompasses both the highest and northernmost land in the United States. It accumulates snow and ice from October to April of each year, which melts in April, producing a large hydrological mass flux as groundwater releases and glaciers surge. Many GPS stations anchored on bedrock throughout the state oscillate vertically by up to 2cm/yr. In addition, the southern part of Alaska is currently being compressed by the Aleutian and Yakutat subduction zones. The deformation is concentrated within a few hundred kilometres of the continental margin. GPS data is being used to track both strain accumulation and mantle movement under Anchorage and the Alaska range (Verner, Finzel and Flesch, 2012). Seasonal motions obscure tectonic signals in both gravity and GPS measurements.

Vertical seasonal movements of southern Alaska due to snow and glacier loading have been studied by Fu, Freymueller and Jensen (2012). They found that their region of study, which covered sixty-four stations between Juneau and Anchorage, moved downwards during the winter and was consistent with GRACE estimates for mass fluxes in the region (readers unfamiliar with the geography of the area may refer to Fig. B-1 in the appendix). All stations in their study are in phase with one another: they all reach their highest point in October and move downwards throughout the

snowy winter season. The time series in Fig. 1-1 is typical for this region. Valdez, one of the snowiest coastal cities in the world, receives an average yearly snowfall of 5.58m (WRCC, 2005). Snowfall typically begins in October, the month when the regions GPS stations begin to lower. Snow depth increases steadily until melting begins in March and April, and indeed in April the GPS stations stop lowering and begin to slowly rise. When we look at the rest of the state, however, the motion is not nearly so consistent.

Fig. 2-2 shows the phases of vertical seasonal motion for forty-eight stations across Alaska. Six stations from Washington state and one from northern Idaho have been included to create a more complete picture of the Northwest; other selection criterion and a full list of stations are given in Appendix A. As described above, stations in the southeast are all in phase, peaking in October.

The full range of phases and amplitudes is shown in Fig. 2-1. Phases are expressed in terms of the date when a station reaches the highest point in its seasonal motion. The average station reaches its highest point on October 4th, as shown by figures of station AB44. However, the range of phases is slightly more than six months. The station with the largest amplitude, AB12, moves with an amplitude of 18.5mm and reaches its highest point on February 5th. It appears to move upwards during the snowy sesason. Some stations, such as AB46, which peaks on July 30, are out of phase with the snow in the opposite direction.

The phase of snowfall varies by only one month across Alaska (WRCC, 2005). Other factors must be driving the apparent seasonal motions of the stations which are out of phase.

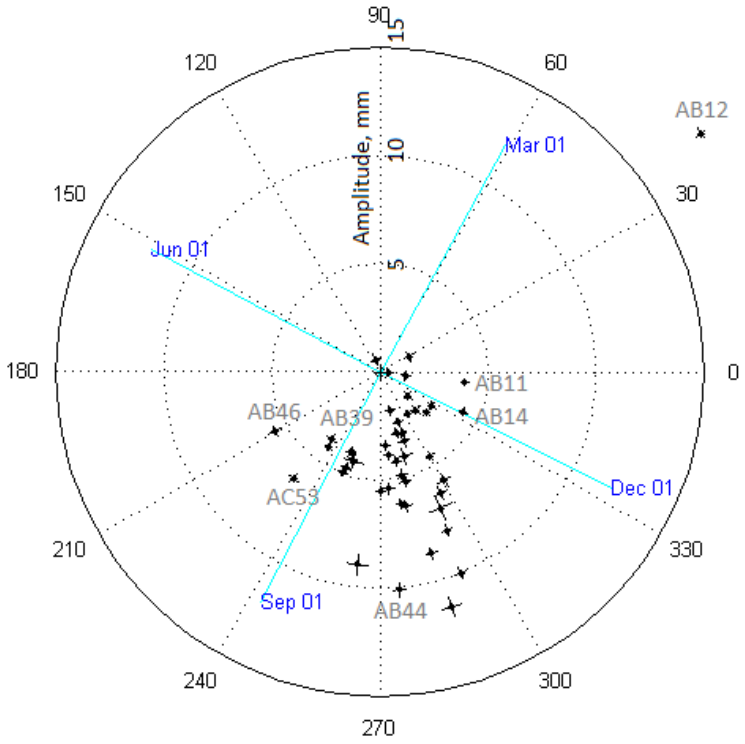

Figure 2-1: Phases and magnitudes (radial) of vertical seasonal variations of 50 GPS stations in Alaska and Washington.

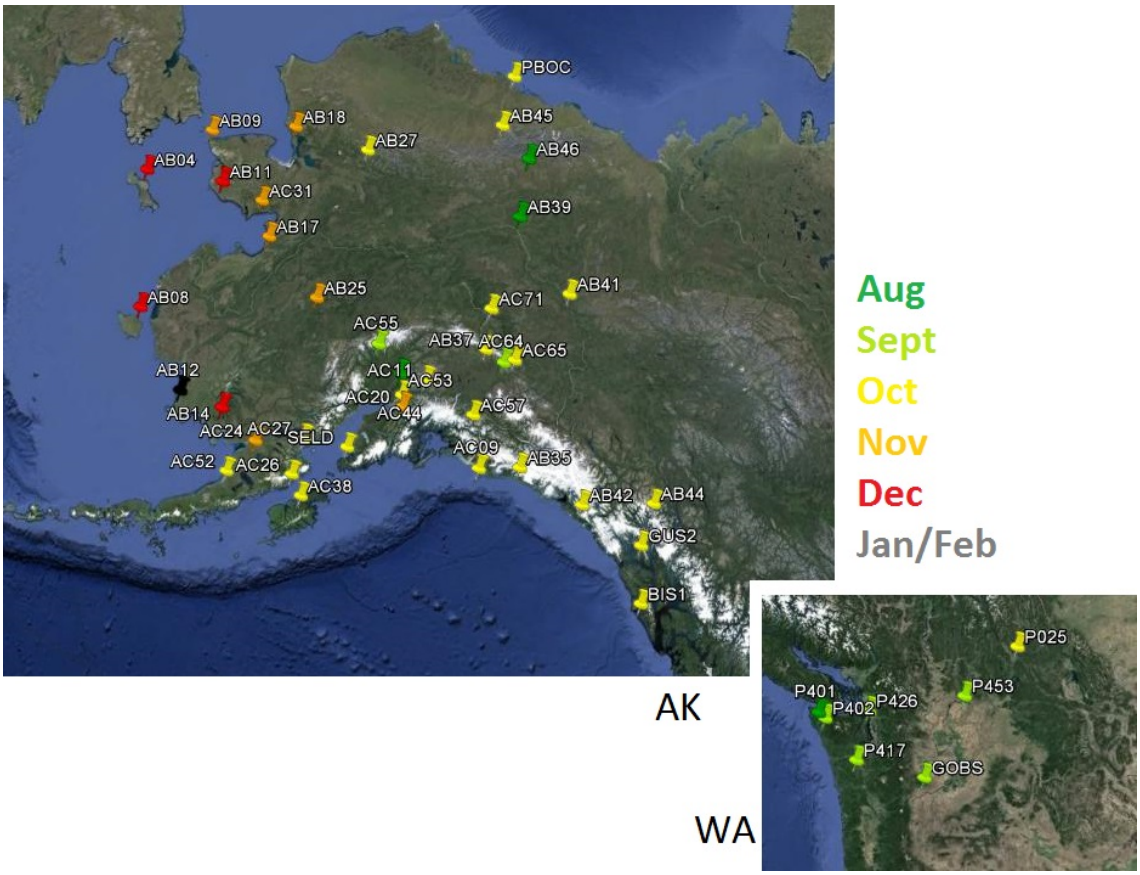

Figure 2-2: 48 GPS stations in Alaska and Washington colored by the phase of their vertical seasonal variations. Image credit: Google Earth.

Chapter 3

Continuous and discontinuous seasonal variations

Seasonal variations do not always have sinusoidal forms. Fig. 3-1 shows the vertical displacement of station AB12. This station has both the latest phase of those studied, peaking on February 5, and an exceptionally large amplitude. A sine function fitted to time series has an amplitude of 18.5mm, but at the extremes of its motion the station moves through over 45mm per year. This time-series appears to have two modes: a summer mode in which position is consistently low, and a winter mode characterised by fast vertical displacements and a higher average position. Looking through the vertical time-series for the other stations in this study, we find six stations which have discontinuous behaviour and shifted positions during each winter season:

AB11 AB12 AB14	Stations move discontinuously up in the winter
AB39 AC53 AB46	Stations move discontinuously down in the winter

AB12 has the most dramatic seasonal movement. AB39 is least dramatic: it shifts

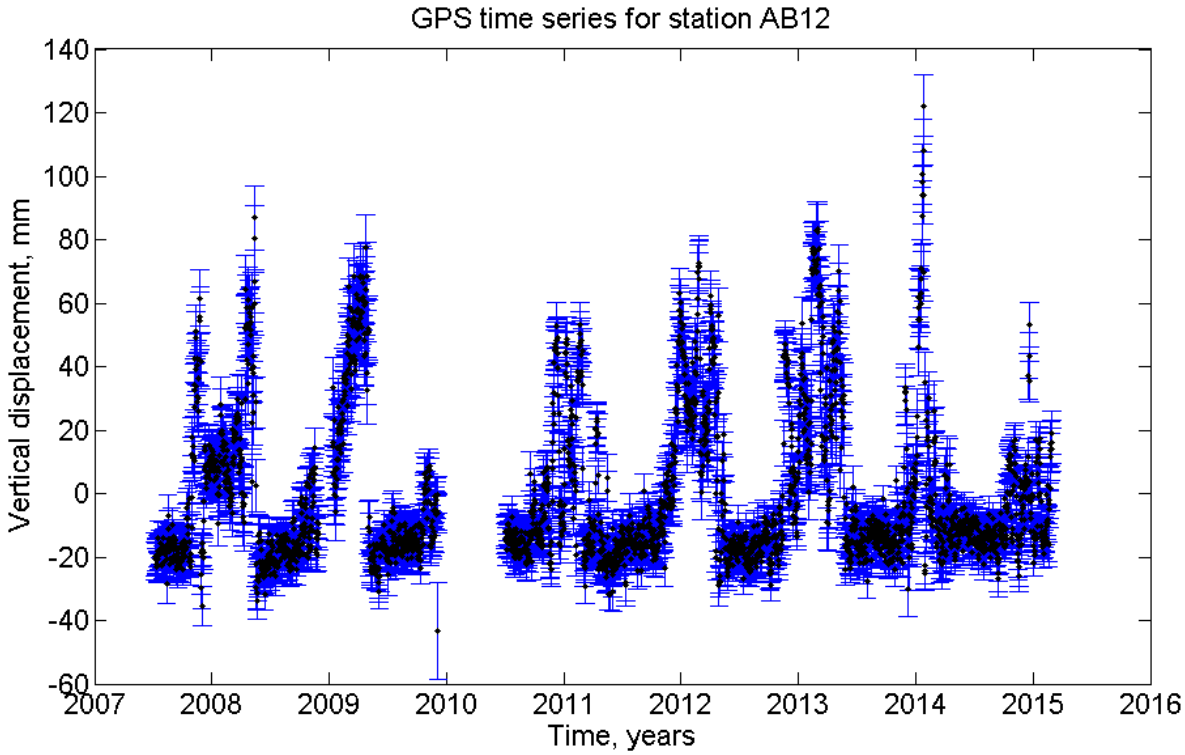

Figure 3-1: Detrended time-series for vertical motion of station AB12.

down by 25mm in 2011, but it moves less in other years and has an average amplitude of only 3.9mm. The three stations which are high during the winter all have spring-shifted phases, peaking in December through February, while the three which are low in the winter all have summer-shifted phases and peak in July and August.

3.1 Skewness and asymmetry of vertical position time-series

These discontinuous distributions are visibly asymmetric. Stationary GPS stations usually return symmetric normally distributed data (Tiberius & Borre, 2000), and sinusoidal seasonal motions are not skewed (Appendix C). The asymmetry of a distribution is measured by its skewness (γ, dimensionless). Skewness is the expected

value (E) of the third moment of a distribution:

$$\gamma = \mathrm{E}\left[\left(\frac{x-\mu}{\sigma}\right)^3\right] \tag{3.1}$$

Here μ is the mean of the distribution and σ is the standard deviation.

The measurements in GPS time series have variable uncertainties. If we calculate the time series' parameters using unweighted sums, the results are strongly skewed by outliers. This effect is immediately visible if we calculate the unweighted skews using all data points and if we do the same calculations after excluding measurements taken within a month of station installations or failures. In the first case, eight stations appear to skews larger than 10. In the second, these large skews all drop by at least half. It is clear that some short periods with extremely irregular measurements distort the stations' apparent movements.

PBO provides uncertainty estimates for each data point. These are calculated from the spread of measurements taken that day and from changes in the phase differences between signals. To accurately estimate the expected values of parameters like skewness and standard deviation for a sample of measurements with changing uncertainty, we can find our parameters using use least-squares fits. For example, the mean (μ) of a sample where each data point x_i has uncertainty δ_i:

$$\mu = \mathrm{E}\left[x\right] = \frac{\sum_{i=1}^{\mathrm{N}} \frac{1}{\delta_i^2} x_i}{\sum_{i=1}^{\mathrm{N}} \frac{1}{\delta_i^2}} \tag{3.2}$$

We can likewise calculate the standard deviation σ of N points:

$$\sigma^2 = \mathrm{E}\left[(x_i-\mu)^2\right] = \frac{\mathrm{N}-1}{\mathrm{N}} \frac{\sum_{i=1}^{\mathrm{N}} \left(\frac{1}{\delta_i^2}\left(x_i-\mu\right)\right)^2}{\sum_{i=1}^{\mathrm{N}} \left(\frac{1}{\delta_i^2}\right)^2} \tag{3.3}$$

The factor of $\frac{\mathrm{N}-1}{\mathrm{N}}$ estimates the population standard deviation of signals at a station from the available data. Finally, using those values for μ and σ, we can calculate the

skew:

$$\gamma^3 = \mathrm{E}\left[\left(\frac{x-\mu}{\sigma}\right)^3\right] = \frac{\sum_{i=1}^{\mathrm{N}}\left(\frac{1}{\delta_i^2}\left(x_i-\mu\right)\right)^3}{\sigma^3\sum_{i=1}^{\mathrm{N}}\left(\frac{1}{\delta_i^2}\right)^3} \tag{3.4}$$

Most stations have skews with magnitudes less than 0.5, but the six stations identified

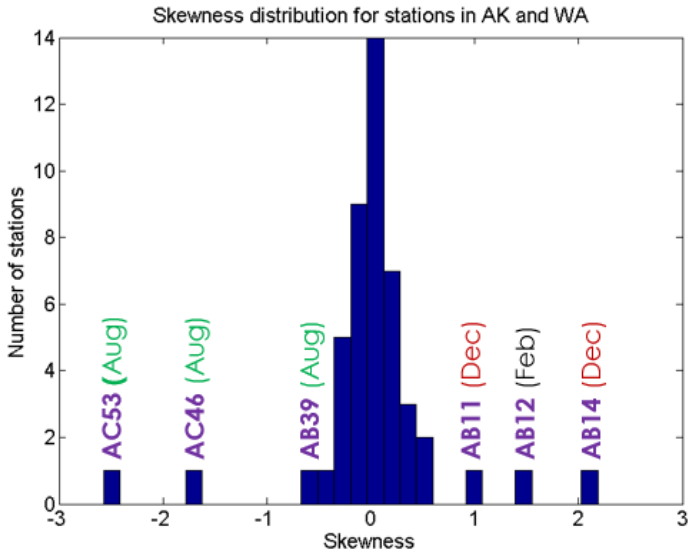

Figure 3-2: Skewnesses of vertical time-series for forty-eight GPS stations in Alaska. Stations with skewness magnitude greater than 0.5 are labelled.

for shifted behavior have unusally larger skews. The sign of the skew is associated with the direction of the winter movement. Appendix C explains the choice of a threshold at ± 0.5 and the mathematical causes of skew in periodic signals.

3.2 Skewness of horizontal position time-series

So far we have discussed only the vertical component of GPS station displacements. Stations move seasonally in the horizontal as well as the vertical directions. The magnitudes of these skews are shown in Fig. 3-3. If the skew-causing apparent motions are caused by seasonal loading (hydrological, atmospheric, or otherwise), we would expect the stations to be tilted slightly towards the center of the load during

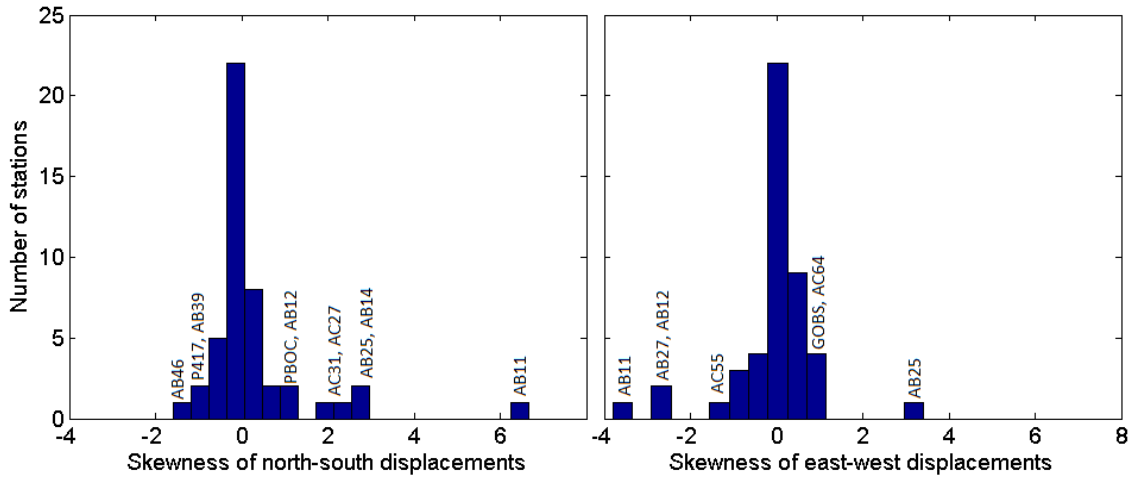

Figure 3-3: Skewnesses of horizontal time-series for forty-eight GPS stations in Alaska. Stations with skewness magnitude greater than 1 are labelled.

the winter months. The horizontal and vertical skews are only loosely correlated. The stations with large horizontal skews, such as AB25 and AC27, have some discontinuous motions in their vertical time-series, but these only appear in select years. Moreover, we can see that the horizontal skewnesses for a single station change from year to year. This is shown for two stations in Fig. 3-4. On this figure, axis scales and dots indicate reported position of the station on each date. Dashed lines indicate the direction and relative magnitude of skew in each year. Years begin on the dates indicated in the legends.

Hydrological loads in Alaska can vary substantially over short distances as weather and drainage patterns are effected by steep mountain ranges which stretch to the coasts. Fu, Freymueller and Jensen (2012) said that this was their biggest limitation, as the GRACE data they used did not always have sufficiently high resolution to localise seasonal loads. If loading is the source of horizontal skews, however, we would still expect it to be consistent from year to year. We would also expect horizontal displacements to be slightly smaller than vertical displacements, which is not the case. During the winter season, horizontal displacements for stations like AB12 are highly variable. They may change direction entirely over the course of a season, and they are often larger than vertical displacements. This is not consistent with expectations

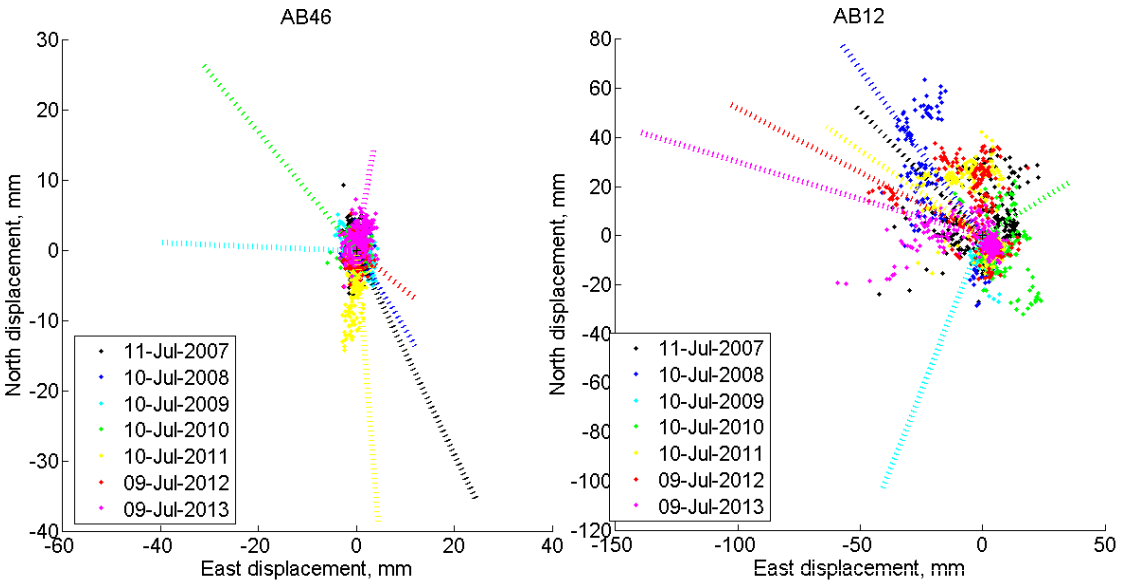

Figure 3-4: Plot of horizontal skewness of each year of data for stations AB12 and AB46.

for a fixed or a gradually changing load.

Chapter 4

Geography of stations with large skewnesses

4.1 Positively skewed stations sit on high points near the Bering Sea

Positively skewed stations AB11, AB12 and AB14 have elevations of 349, 587 and 658m respectively. AB11 and AB12 are within 2km of the coast, and AB14 is separated from the ocean by 40km of low-lying terrain. Their elevations are not remarkable - the highest station in this study, AB37, is at 1137m, and even that is a small fraction of the heights of the Brooks and Alaska Ranges - but all three stations are anchored in bare bedrock on local high points. These locations are exceptionally exposed, unsheltered from the wind and weather of the Bering Sea.

Alaska, of course, contains many exposed locations. But almost none of them contain GPS stations. Thirteen stations in this study are located on Alaska's west coast, and all but four of them - AB09, AB11, AB12 and AB14 - sit nearly at sea level. AB09 is the only high point on the Bering Sea that does not have significant skew ($\gamma_{AB09} = 0.233$). It has a slightly lower elevation than the skewed stations, 162m, is on the very western tip of the Seward Peninsula. Two stations (AC09, AC35) on the

edge of the Gulf of Alaska, in the southeast of the state, also have high elevations but small skews. The south of the state general experiences weaker winds (NREL, 2015). All told, 7 stations in this study are on high points or ridges (AB09, AB11, AB12, AB14, AB25, AB27, AC55). Their mean skewness is +0.81 (or +0.25 neglecting the three highest skews) and three of them - all near the Bering Sea - have skewnesses greater than +1/. In contrast, the 41 stations in valleys, estuaries, fjords and flatland have a mean skewness of −0.13.

4.2 The three most negatively-skewed stations are in deep valleys

AB39 is in a small valley just south of the Brooks Range. AB46 is next to the Yukon river in the bottom of a large low-lying area of Alaska's interior. AC53 has an elevation of 57m in a floodplain near Anchorage. These three stations are all next to rivers which drain large, snowy mountain ranges. Five other stations are next to major rivers. Two of them, AB41 and AB71, behave discontinuously in a single year; the others (AC20, PBOC and AC65) are not visibly irregular. These river stations have a mean skew of −0.70, or −0.11 discounting the three most negative skews.

4.3 Known causes of skewness in GPS time-series

Previous works have found skewness in GPS time-series caused by various weather and scattering effects. Hydrological loading is not usually associated with skewness of GPS signals, and none of the Alaskan stations whose hydrologically-driven variation was investigated Fu, Freymueller, & Jensen,(2012) had significant skewness. Materna and Herring (2013) measured skewness and apparent motions caused by gravity waves

in the atmosphere. This phenomenon occurs when high winds pass over steep mountains. Some of the stations in Alaska, including but not limited to AB46 and AB39, are in deep valleys which and could experience gravity waves. Skew due to gravity waves, however, occurs on individual windy days rather than persisting throughout a season. Jaldehag et. al. (1996a) found skewness in high-latitude Swedish GPS stations due to scatter off the equipment. This effect is not seasonal in itself, but seasonal accumulation of reflective ice or snow around the station could increase the strength of the effect in winter.

Scattering can be detected because scattered signals reach the GPS station by different paths with different phases, increasing the signal's multipath value (Bilich & Larson, 2007). Multipath values are shown over the course of a year for two skewed stations in Fig. 4-1. Dark red and light blue lines indicate multipath values for frequencies L1 and L2 respectively. These are representative for stations with positive and negative vertical skew. Positively skewed stations like AB12 have increased multipath values during the winter, beginning at the same time the station shifts upwards. Multipath values increase more for the signal with the higher frequency, L1, than for the lower frequency L2. This would be the expected result for a signal which is refracted through ice or water, in which high frequency signals are attenuated more than low frequency signals (this effect was verified for GPS signals by O'Keefe, Lachapelle & Gonzales, 2000). The multipath values for negatively-skewed station AB46, however, do not appear to change seasonally. These observations are characteristic of all six vertically-skewed stations for all the years on record. The multipath values do not explain the stations with negative skews, but they are good evidence that the positive skewnesses of stations AB11, AB12 and AB14 are caused by scattering rather than physical motion.

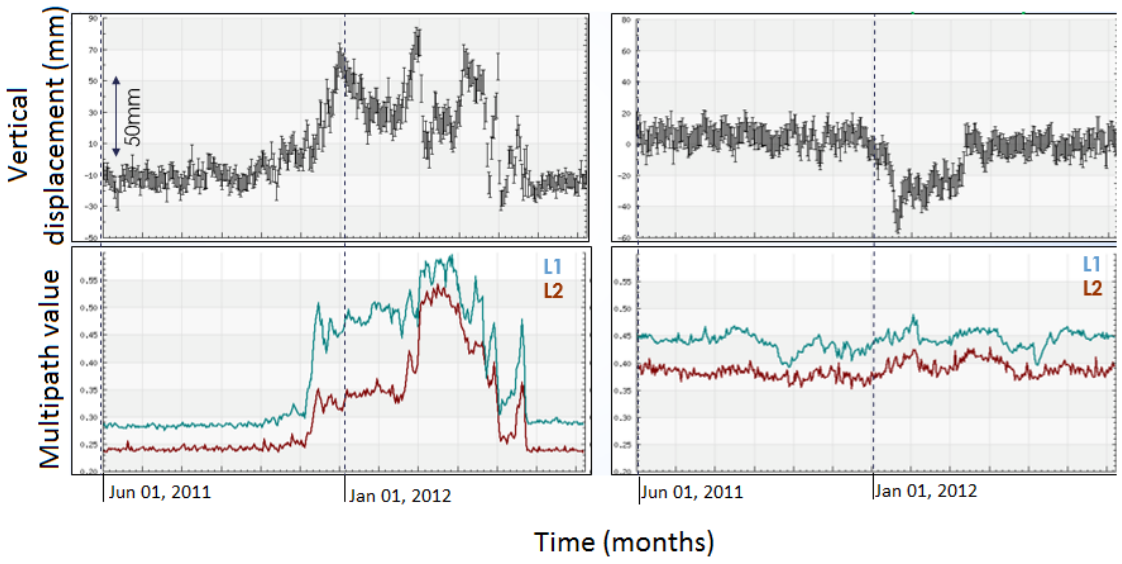

Figure 4-1: Variation of vertical position (upper plots) and multipath values (lower plots) over the course of one year for stations AB12 and AB46.

Chapter 5

Ice accumulation and apparent variations in GPS position

Accumulated frost and ice is very likely to cause scattering on GPS stations in northern latitudes. We have already seen that many of the skewed stations have very damp and exposed locations, where the wind will deposit rime ice, and that others are in valleys which may accumulate deep snow.

O'Keefe et. al. (2000) investigated of the effect of rime on GPS signals by placing ice cones on a GPS antenna and observing the changes in its signal and apparent position. They found that water and wet ice attenuated the GPS signal rapidly (with decay lengths of 3.9cm for frequency L1 and 6.4cm for L2). Dry ice - such as the ice in rime deposited at temperatures far below freezing - attenuated the signal by much less, with longer decay lengths of 31.7m for L1 and L2. Because decay lengths are the length scale for exponential decay, the difference in signal strengths is very substantial: frequency L1 will be attenuated by 3.11% after travelling through a meter of dry ice, but will be attenuated by 99.5% after travelling through only 20cm of water. Because GPS signals are not noticeably attenuated in dry ice, the signals may not be noticeably weak and the distortion is less likely to be observable in the data.

GPS signals are scattered when they interact with irregular ice surfaces, however.

Rime ice is typically deposited in thick feather-like structures. These would refract signals and increase the multipath value as seen for station AB12 in Fig. 4-1.

Previous work by Jaldehag et. al. (1996b) has documented apparent upwards displacement of Swedish GPS stations during the winter. They correlated the effect with precipitation records and concluded that it was a positioning error created by snow accumulation. This argument was supported by a theoretical calculation of estimated position for a conical GPS radome covered in snow.

5.1 Model for rime accumulation on GPS stations

We built a simple simulation to demonstrate the effect of rime accumulation on GPS station position estimates. Rime is deposited asymmetrically, unlike the snow in Jaldehag's model, and is more likely to accumulate in windswept sites. The geometry used in our model is shown in Fig. 5-1. The rime creates a maximum signal delay $\Delta\tau_0$ at an azimuthal angle of θ_r. The signal delay $\Delta\tau_{rime}$ around the rest of an antenna is:

$$\Delta\tau_{rime} = \begin{Bmatrix} T_0 \cos(\alpha - \theta_r)(\frac{\pi}{2} - \epsilon) & \frac{-\pi}{2} \leq \alpha - \theta_r < \frac{\pi}{2} \\ 0 & else \end{Bmatrix} \tag{5.1}$$

Real rime has irregular, feather-like geometry and an anisotropic interior structure.

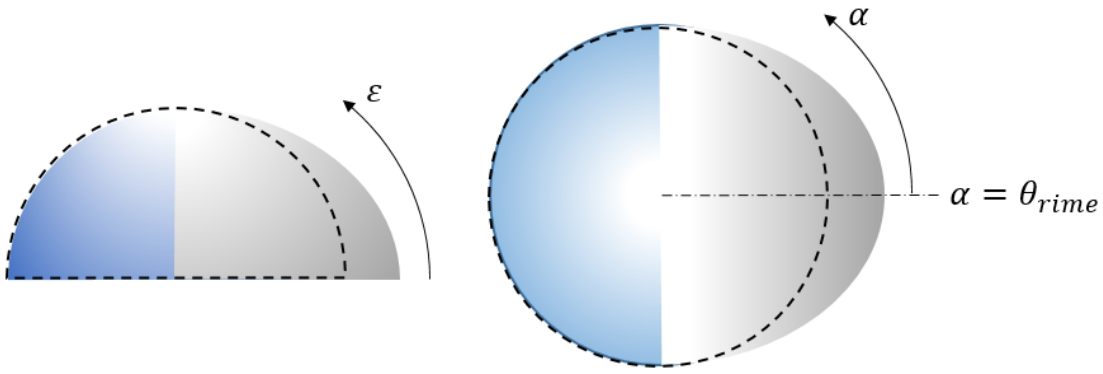

Figure 5-1: Rime geometry used in simulation.

The formation of rime has never been modelled, however, so this model attempts to

capture two crucial features : the hemispherical shape of PBO antennae, and the asymmetry of the accumulated ice.

5.2 Station position as a function of signal delay

To calculate its position, GPS stations receive several signals from satellites. In normal conditions, the time it takes a signal to travel from a satellite ($\Delta\tau$) to a GPS station is a function of its three position coordinates (vertical z, east x and north y), as well as an atmospheric delay proportional to the thickness of the atmosphere in its direction of travel, and a clock error ($\Delta\tau_{clock}$) which corrects for differences in the station's and the satellite's time-keeping. The relative importance of each of these displacements is a function of the satellites' position, measured according to its elevation (ϵ) and azimuthal (α) angles in the sky.

$$\begin{aligned} \Delta\tau &= -\Delta z \sin\epsilon + \Delta y \cos\epsilon \cos\alpha \\ &\quad + \Delta x \cos\epsilon \sin\alpha + \Delta\tau_{clock} + \Delta A_{tm}(\sin\epsilon + c) \end{aligned} \tag{5.2}$$

This equation is underspecified, so to calculate the station's position it is necessary to take measurements of $\Delta\tau$ from at least five satellites (or five points along a satellite's trajectory). The number of possible measurements is limited by the number of satellites visible in the sky, and the decorrelation time of noise in the signal. GPS stations normally take measurements ever fifteen seconds from each satellite in their range.

5.3 GPS satellite paths over Alaska

Fig. 5-2 shows typical paths followed by GPS satellites. These satellites' orbits do not cross the poles, so the satellites' trajectories around high-latitude GPS stations are asymmetric, with low elevation angles. A sample trace of these satellite paths around station AB11 , at 64.5°N 165.4°W (marked on Fig. 5-2, is shown in Fig. 5-3. In this figure the azimuthal angle progresses counter-clockwise, from north at the bottom of the figure towards east at the left.

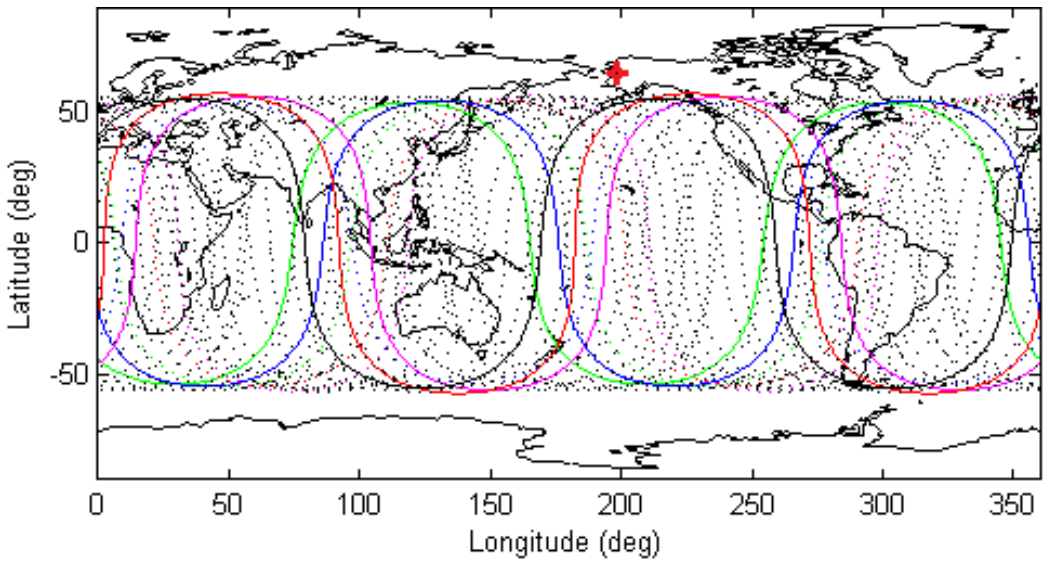

Figure 5-2: Trace of GPS satellite paths over the Earth. Figure credit T. Herring.

The Swedish permanent GPS network, operating at nearly identical latitudes to those in our study, found that the geometry of satellite paths created skewness and apparent displacements of their station. This was confirmed by Jaldehag et. al. (1996a) who found that the apparent position of their satellites changed by as much as $22.3 \pm 1.6mm$ vertically and more than 5mm north when they changed the elevation angle cut-off from 10° to 20°. They attributed these errors to the scattering of low-elevation angle signals off the GPS structure. The effects of elevation angle cut-offs will be more pronounced for stations which are in valleys or fjords where mountains block parts of the sky than for stations on high points.

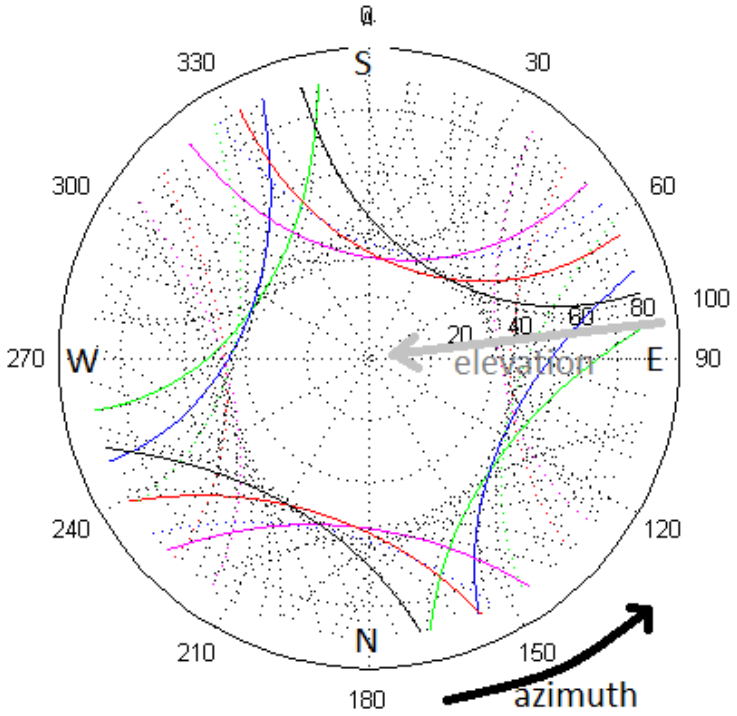

Figure 5-3: Trace of GPS satellite paths in the sky over station AB11. Figure credit T. Herring.

5.4 Simulation results for apparent position as a function of ice angle

We calculated rime-caused apparent displacement for seventy-two values of θ_r. For each value, we used Eqn. 5.1 to calculate the expected signal delay for each point on the satellite paths shown in Fig. 5-3 with an elevation angle greater than 10°, then performed a least-squares fit to estimate the displacements, clock error and atmospheric delay. The results are shown in Fig. 5-4.

These results show that, even with a simplified geometry, rime accumulation can cause large vertical displacements. The rime delay is given in dimensionless units.

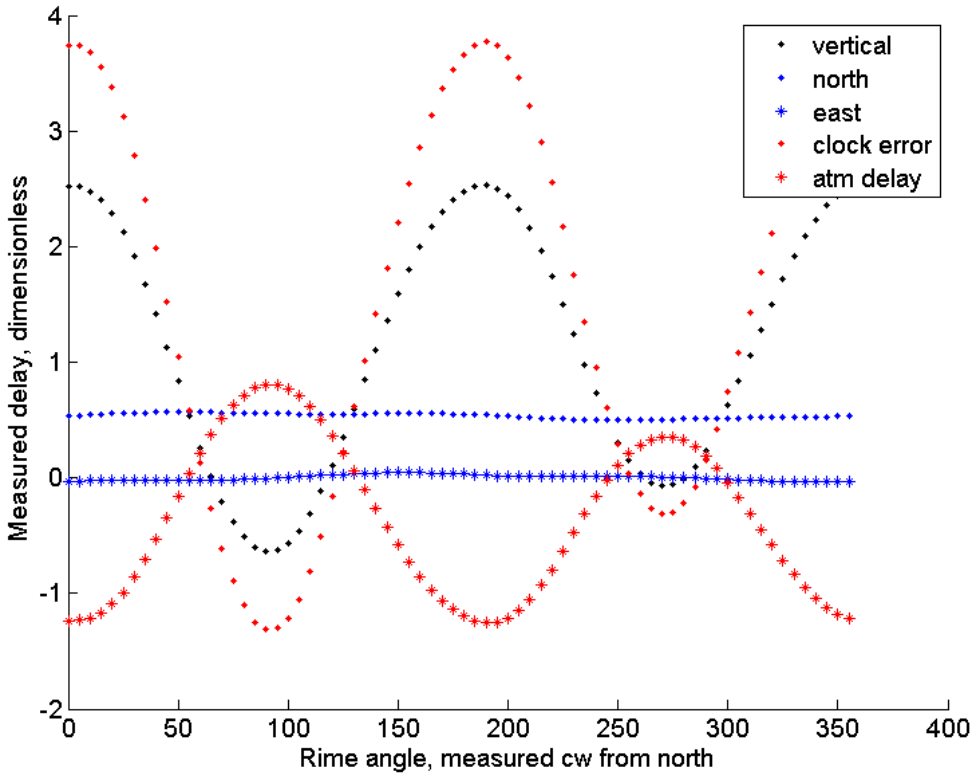

Figure 5-4: Apparent position of a GPS station as a function of rime angle.

Actual delays would be determined by rime thickness multiplied by a delay rate which will be a function of the rime density.

5.5 Rime angle is a function of wind direction

Rime forms when humid air is blown into a cold object and freezes there. We can therefore approximate θ_r at a given location if we know the typical wind direction. Rime accumulation rates are a poorly-constrained function of wind speed, temperature and humidity, so we will not attempt to move beyond the approximate dimensionless delays estimated in Fig. 5-4.

Wind speed measurements for the three positively skewed stations are shown in Fig. 5-5. All three stations have consistent wind directions between 16° (AB11) and 79° (AB14) measured cw from north. If we compare these values with the results from Fig. 5-4, we find that the wind directions at AB11 and AB12 are consistent with apparent vertical motion up. This is what we observe at these stations during the winter. For AB14, however, we predicted a slight downwards vertical motion. The wind direction measurements may be straining the limited precision of our model, or the wind directions used may be inaccurate for the stations' locations: all sets of wind data were taken from airport weather stations, but AB14 is 340m above and 13km north of the nearest weather station. Bearings are measured clockwise from north, and wind speeds are in mph. Measurements were taken for the same dates on the GPS station records.

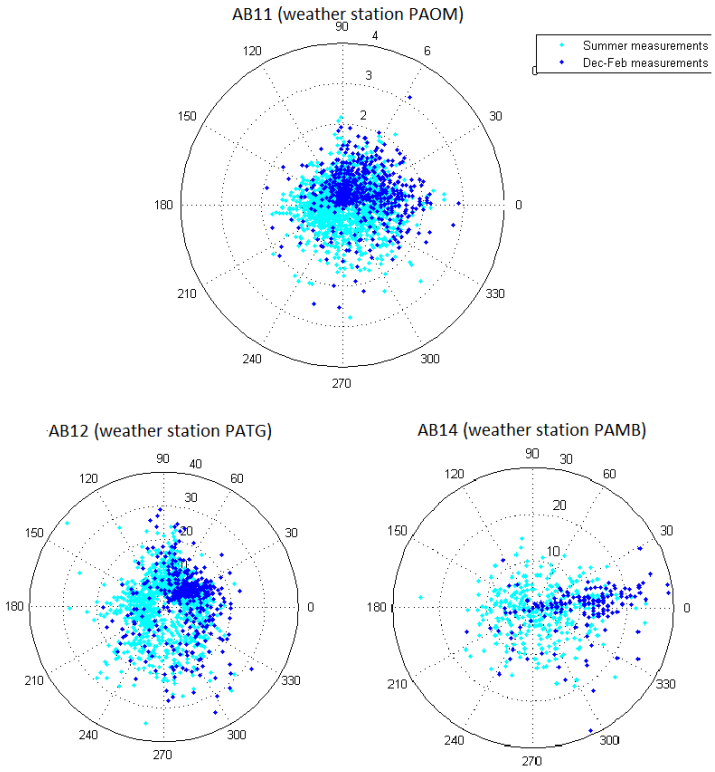

Figure 5-5: Wind speed and direction for weather stations nearest GPS stations AB11, AB12 and AB14. See Weather Underground (2015a,b,c).

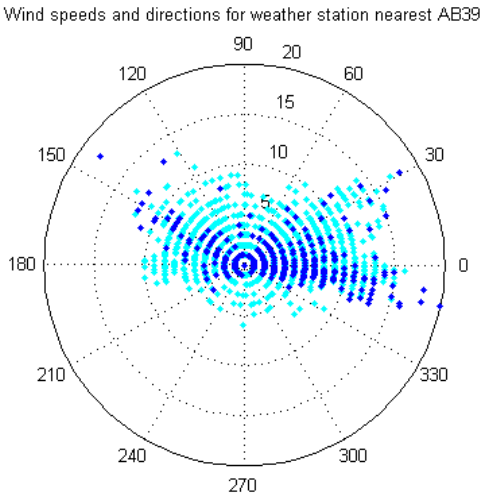

Figure 5-6: Wind speed and direction measurements at Fort Yukon airport, location of station AB39. See Weather Underground (2015d).

Weather data for the negatively skewed stations is even sparser because of their remote locations in the state's interior. Station AB39 is located at Fort Yukon airport, which also maintains a weather station. Its wind speed history is shown in Fig. 5-6. Stations AB41 and AC53, however, are both separated from the nearest weather station by over 40km of rough terrain. Reanalysis data for weather histories is available in the area, but as the two stations are both located in valleys, these 5km grids are unlikely to be sufficiently precise. AB39 has two major wind directions in winter, both of which would create rime at angles for which our model predicted apparent motion down.

Rime accumulates only at temperatures below freezing, and collapses rapidly when temperatures increase. Rime plumes in exposed locations can reach lengths of centimeters to meters if left undisturbed.

Chapter 6

Discussion

At least six stations in Alaska have systematic position offsets caused by large seasonal variations. Three stations, AB11, AB12 and AB14, move systematically up each winter. The time-series of these stations have significant positive skew, and the published multipath values for these stations indicate elevated signal scattering during the winter months.

We propose that these disruptions are caused by the accumulation of rime on the stations. This conclusion is drawn from the exposed locations of the stations - all on rocky, windswept hills near the edge of the Bering Sea - and from simulations indicating that rime accumulation on Alaskan satellites can cause apparent upwards motion. Apparent vertical motion in winter was also been observed in the Swedish permanent GPS network and was attributed to snow accumulation by Jaldehag et. al. (1996b).

These apparent seasonal variations are as large as 10cm per season. The motions are discontinuous and do not appear to be caused by physical processes such as loading. They add significant noise to the data and create a persistent offset in position estimates, as well as completely obscuring any seasonal variations due to hydrological or tidal loading.

The simulation presented in Fig. 5-4 does not attempt to estimate the magnitude of apparent motion. Accurate estimates would require more detailed knowledge of rime thickness and density than is currently available. In addition, this result does not adequately explain the large skews observed in the horizontal time series of some stations. In that simulation, we used single values for atmospheric and clock delays and did not attempt to calculate independent values for each GPS satellite in the sky. This may have made the results unrealistically symmetric.

The presence of rime could be confirmed periodically photographing the stations, thus capturing the appearance and growth of ice. Cameras are unreliable in wet winter conditions, but would be far less difficult or expensive than winter field visits. They would also provide useful estimates for rime magnitude. Imaging winter conditions on GPS stations might also reveal causes of skew and scattering that were not examined in this study.

Another three stations, AB39, AB46 and AC53, move systematically down each winter and have time series with significant negative skew. Our simulations indicate that rime can cause slight apparent downwards movement if it forms pointing towards the east or west. These three stations are located in remote, low-lying areas without nearby weather stations, making it difficult to remotely estimate their winter ice conditions. In addition, their multipath values do not increase seasonally, so there is no clear evidence that signals from these stations are being reflected from ice.

Appendix A

Appendix A: GPS stations used in this study

All stations are part of the Plate Boundary Observatory network. Data is provided by UNAVCO. Stations were selected to provide an even geographical spread across Alaska. All stations in this study have at least four years of continuous data (all but one have at least five years), uninterrupted by earthquakes or nearby volcanic activity, and no maintenance failures which went unrepaired for longer than one season.

GPS stations used in this study							
AB04	AB08	AB09	AB11	AB12	AB14	AB17	AB18
AB25	AB27	AB35	AB37	AB39	AB41	AB42	AB44
AB45	AB46	AC09	AC11	AC13	AC15	AC20	AC24
AC26	AC27	AC31	AC38	AC44	AC52	AC53	AC55
AC57	AC58	AC64	AC65	AC71	BIS1	GOBS	GUS2
P025	P401	P402	P417	P426	P453	PBOC	SELD

Appendix B

Appendix B : Reference map

This appendix provides a reference map for readers unfamiliar with the geography of Alaska and the Northwest. Distances on this map projection are not proportional to distances on the ground.

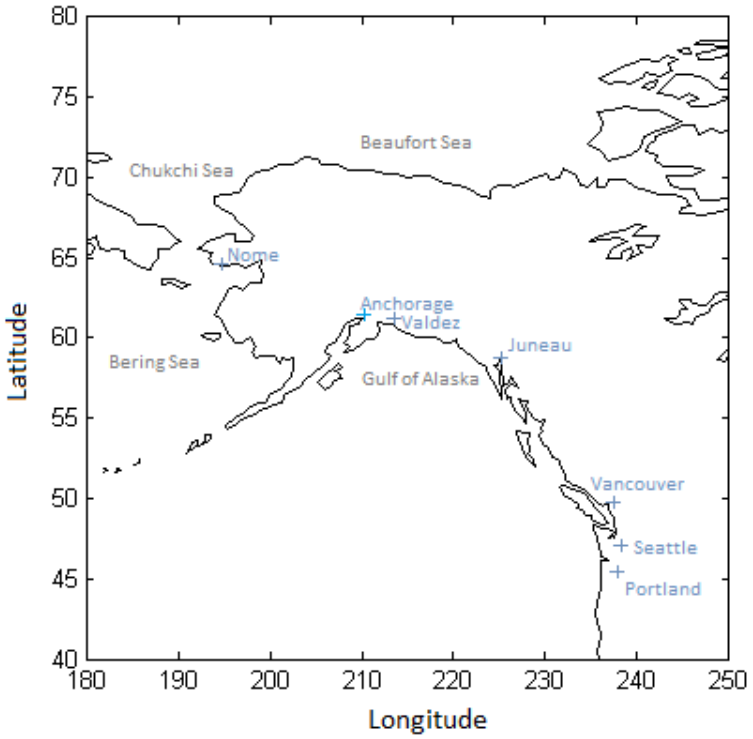

Figure B-1: Seas and major cities of Alaska, Washington and British Columbia.

Appendix C

Appendix C : Skewness of periodic functions

In Fig. 3-2 we saw that most time series have non-zero skews between -0.5 and $+0.5$. We neglected these small skews in the main body of the analysis. The justifications for this cut-off, and two likely causes of small skews, are given below.

In section III, we used skewness to identify unusually asymmetric functions. This result relies on the fact that sinusoidal functions have skewness (γ) of zero. This can be demonstrated using the skewness formula from Eqn. 3.1 to calculate the skew of a sine function over a single period:

$$\gamma^3 = \frac{1}{\sigma^3} \int_0^{2\pi} \cos^3(t) \mathrm{d}t = 0 \tag{C.1}$$

C.1 Skew from partial periods

In Fig. 3-2 we saw that most time series have non-zero skews between -0.5 and $+0.5$. Sinusoidal seasonal functions can have non-zero skews for two reasons. First, our integral in Eqn. C.1 used a signal length was exactly one period, but time series do not cover an exact number of years. The skew of a sinusoidal function with a signal length of a periods, or a time series with length a years, can be calculated as

follows:

$$\gamma^3 = \frac{1}{2\pi a \sigma^3} \int_0^{2\pi a} \cos^3(t) \mathrm{d}t = \frac{1}{24\pi a \sigma^3} \left(9\sin(2\pi a) + \sin(6\pi a)\right) \tag{C.2}$$

The standard deviation σ for this function is:

$$\sigma^2 = \frac{1}{2\pi a} \int_0^{2\pi a} \cos^2(t) \mathrm{d}t = \frac{1}{2} + \frac{1}{8\pi a} \sin(4\pi a) \tag{C.3}$$

The skewness γ can be calculated by substituting the result from Eqn. C.3 into C.2. The result is shown as a function of a in Fig. C-1. This result makes the small approximation that signal's mean was zero regardless of the signal length. All of the GPS stations used in this paper had at least four years worth of data, so we are only concerned with parts of the graph where $a > 4$. Over this length, varying the period creates a skew of up to ± 0.08, and the magnitude of the skew decreases as the length of the signal increases. Fig. C-2 compares the results in Fig. C-1 to the skewnesses of

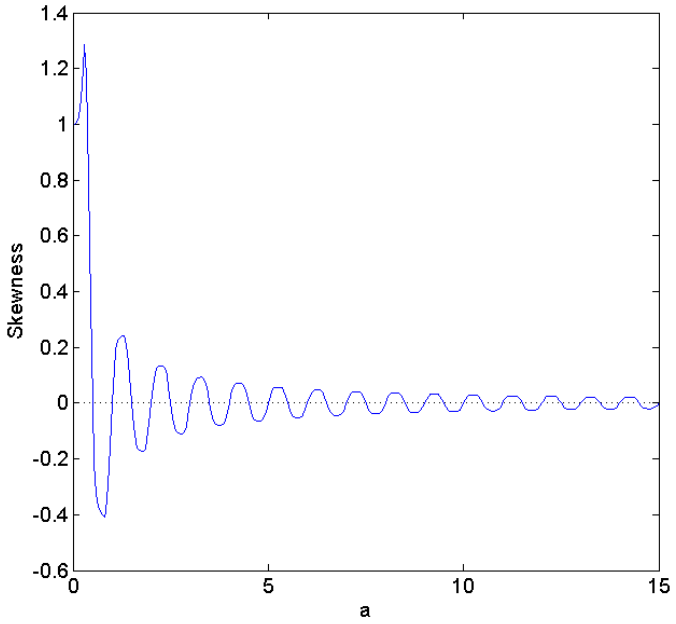

Figure C-1: Variation of skewness of a sinusoidal signal with signal length.

GPS stations' vertical time-series. This analysis could be cross-checked by trimming all of the time-series to whole numbers of years, then repeating the skew calculations.

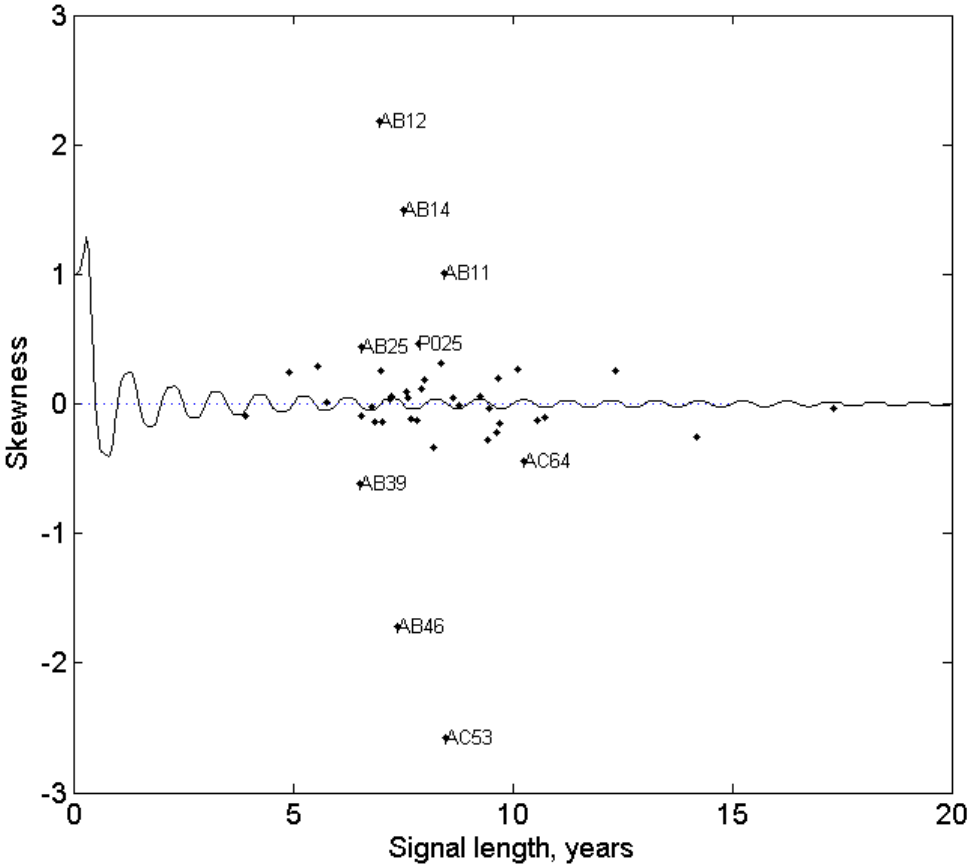

Figure C-2: Skewness of GPS station vertical time series as a function of signal length.

However as the magnitude of skews created by changing the signal length is significantly smaller than our skew cut-off, we neglected them in favor of using all our data.

C.2 Skew from semi-annual signal components

Seasonal variations in GPS time-series usually have both an annual and a semi-annual component. So far we have neglected the semi-annual component This signal appeared as a smaller peak in the time-series fourier transform in Fig. 1-2, and has also been observed by authors including Dong et. al. (2002). The following derivation demon-

strates how an additional frequency signal can create skew in a periodic function. We will not discuss higher frequencies, assuming that they appear in GPS signals with small amplitudes and random phases. Higher frequencies are course present in the form of noise and make small, non-systematic contributions to the skew.

A signal (x) with two frequency components, one twice as high as the other (for example an annual and a semi-annual signal), takes the following form:

$$x(t) = \sin(t) + A\sin(2t + \phi) \tag{C.4}$$

where A is the ratio of the amplitudes of the two signal components and ϕ is a phase offset. For simplicity we will assume that the signal length is an integer number of periods, i.e. $a = n$ for $n \in \mathbb{Z}^+$. Using the same integration method followed in Eqns. C.2 and C.3, and observing that the mean of $x(t)$ is zero, we find:

$$\gamma^3 = \frac{\frac{1}{2n\pi}\int_0^{2n\pi} x(t)^3 \mathrm{d}t}{\left(\frac{1}{2n\pi}\int_0^{2n\pi} x(t)^2 \mathrm{d}t\right)^{3/2}} = \frac{-\frac{3}{4}A\sin(\phi)4\pi}{\frac{1}{2}\left(1 + A^2\right)} \tag{C.5}$$

The greatest skew which can be created from semi-annual signals, when $\sin\phi = -1$, is $\frac{3A^{1/3}}{2(1+A^2)}$. Fourier transforms such as the one shown in 1-2 show that the root mean square value for A for vertical signals is 0.34. This could create a skew as large as 0.45, which is larger than all but five of the observed vertical skews (see Fig. C-2). We observe, however, that the two signals are usually roughly in phase so we can expect a small value for $\sin(\phi)$.

These two processes - partial periods and semi-annual signals - both occur in GPS time-series. THe partial periods cannot make contributions larger than 0.08 to skew over 4-year periods and can be safely neglected in this study. Semi-annual signals, however, are regularly observed in GPS time-series and could reasonably make contributions to skew on the order of 0.7. This potentially explains the distribution of skews in vertical time-series, and justifies the cut-off used to identify abnormally

large skews. Only nine stations (AB11, AB12, AB14, AB25, P025, AB41, AB39, AB46 and AC53) have vertical skews too large to be created by this effect, and three of those (AB25, P025 and AB41) have skews $0.45 < \gamma < 0.5$. However, five stations have skews larger than 1. Creating skews of this size in a periodic function requires large-amplitude signals with higher frequencies (such as very large values of A) than are explained by semi-annual atmospheric effects, but strong high-frequency signals are not observed in spectral analyses of GPS time-series. The system could also be forced annually by some non-linear process which creates the observed discontinuous behaviour, such as signal delays due to ice and snow.

Bibliography

[1] Bilich, A.; Larson, K.M. (2007) *Mapping the GPS multipath environment using the signal-to-noise ration (SNR).* Radio Science 42(6003).

[2] Borsa, A.A.; Agnew, D.C.; Cayan, D.R. (2014) *Ongoing drought-induced uplift in the western United States*, Science 345 (6204): 1587-1590.

[3] Google Earth (2013) *Alaska and Washington state.* 63.7°N, 150.9°W, eye alt 2796km. Image IBCAO, Landsat. Data SIO, NOAA, U.S. Navy, NGA, GEBCO.

[4] Dong, D.; Fang, P.; Cheng, M.K.; Miyazaki, S. (2002) *Anatomy of apparent seasonal variations from GPS-derived site position time series*, J. Geophysical Research, 107 (B4).

[5] Flouzat, M.; Bettinelli, P.; Willis, P.; Avouac, J-P.; Heritier, T.; Gautam, U. (2009) *Investigating tropospheric effects and seasonal position variations in GPS and DORIS time-series in the Nepal Himalaya*, Geophysical Journal International.

[6] Fu, Y.; Freymueller, J.T.; Jensen,T. (2012) *Seasonal hydrological loading in souther Alaska observed by GPS an GRACE*, Geophysical Research Letters, 13-45.

[7] Jaldehag, R.T.K; Johansson, J.M.; Davis, J.L.; Elósegui, P. (1996a) *Geodesy using the Swedish permanent GPS network: Effects of snow accumulation on estimates of site positions.* Geophysical Research Letters 23(13) 1601-1604.

[8] Jaldehag, R.T.K; Rönnäng, B.O.; Elósegui, P.; Davis, J.L.; Shapiro, I.I.; Niell, A.E. (1996b). *Geodesy using the Swedish permanent GPS network: Effects of signal scattering on estimates of relative site positions.* J. Geophysical Research Solid Earth. 10(B8) 17841-17860.

[9] Materna, K.; Herring, T. (2013), *Analysis of skewed GPS position estimates: Effects of coupling local topography and atmospheric conditions.* AGU Fall Meeting abstract.

[10] O'Keefe, K.; Stephen, J.; Lachapelle, G.; Gonzales, R.A. (2000) *Effect of Ice Loading of a GPS Antenna* Geomatica 54(1): 63-74.

[11] Tiberius, C.C.J.M.; Borre, K. (2000). *Are GPS data normally distributed?* International Association of Geodesy Synopsis, 121: 243-248.

[12] Tsai, V.C (2011) *A model for seasonal changes in GPS positions and seismic wave speeds due to thermoelastic and hydrologic variations*, J. Geophysical Research 39, L15310.

[13] Verner, K.; Finzel, E.; Flesch, L. (2012) *Mapping large-scale mantle flow driving surface motions in southern and central Alaska through the integration of GPS and shear-wave splitting data.* AGU Fall Meeting Abstracts (A2343).

[14] NREL)National Renewable Energy Laboratory); Alaska Energy Authority (2015) *Alaska 50m wind power*. Department of Energy.

[15] Weather Underground (2015a) *Weather History for PAOM (Nome, AK)*, wunderground.com. [accessed May 8 2015].

[16] Weather Underground (2015b) *Weather History for PATG (Togiak, AK)*, wunderground.com. [accessed May 8 2015].

[17] Weather Underground (2015c) *Weather history for PAMB (Manokotat, AK)*, wunderground.com [accessed May 8 2015].

[18] Weather Underground (2015d) *Weather History for PFYU (Fort Yukon, AK)*, wunderground.com. [accessed May 8 2015].

[19] WRCC (2005). *Valdez, Alaska, Period of record monthly climate summary.* Western Regional Climate Center, wrcc.dri.edu [accessed 22 May 2015].